PHYSICS AND CHEMISTRY OF SOLID STATE
V. 23, No. 4 (2022) pp. 728-740
Section: Physics

DOI: 10.15330/pcss.23.4.728-740

Vasyl Stefanyk Precarpathian National University

ФІЗИКА І ХІМІЯ ТВЕРДОГО ТІЛА
Т. 23, № 4 (2022) С. 728-740
Фізико-математичні науки

PACS: 31.15.A-; 46.70.-P; 62.20.D-; 62.20.de; 65.40.De; 65.40.-b; 65.60.+a; 71.20.-b ISSN 1729-4428

J. Kumari[1], C. Singh[2], B. L. Choudhary[1] and A. S. Verma[3,4]

First-principles study for physical properties and stability of Li based chalcopyrite semiconductors: Reliable for green energy sources

[1]*Department of Physics, Banasthali Vidyapith, Rajasthan, India,*
[2]*Department of Physics, Agra College, Agra, India,*
[3]*Division of Research & Innovation, Department of Applied and Life Sciences, Uttaranchal University, Dehradun, Uttarakhand, India,*
[4]*University Centre for Research & Development, Department of Physics, Chandigarh University, Mohali, Punjab, India,*
ajay_phy@rediffmail.com

In this research study, we have been performed the first principles calculation for physical properties likewise structural, electronic, optical and mechanical properties of the lithium gallium chalcopyrites $LiGaX_2$ (X= S, Se). We have used two exchange correlation potentials one is full potential augmented plane wave method (FP-LAPW) and second is pseudo-potential method. The reported lattice parameters in this work ranging from a = b = 5.28 Å to 5.82 Å and c = 10.11 Å to 11.25 Å and found that these materials have direct band-gap 4.41 eV for $LiGaS_2$ and 2.90 eV for $LiGaSe_2$. Refractive indexes n(ω) is 2.1 and 2.3 respectively for these compounds. The study of optical and elastic properties for these materials ensures that these show the anisotropic behaviour and ductile in nature.

Keywords: chalcopyrites; electronic properties; optical properties; elastic properties.

Received 09 April 2022; Accepted 30 November 2022.

Introduction

We are very well introduced with the current condition of population of the world, and we can say that our life is completely depends on gadgets, machines, electronics etc. and these things can be operated only by electricity which is a form of energy. Today's world is the world of technology because now days technologies are growing day by day in a rapid speed, according to a study we conclude that the use of electricity is very high as compare to its production which is the reason of energy crisis. So, we need to improve the rate of production of energy. Recently, for resolving this issue many energies are produced from the energy incomes likewise from oil, gas (natural), coal etc. but these are natural incomes of energy and they are existing at our universe in a very limited amount, which are using by human being very fast due to which they will be vanish in few more years. Also, these resources have some disadvantages like when we do the process of production of energy from these resources they affect our environment i.e., cause air pollution, water and soil pollution, also discharging numerous green-house gases which is the big reason of turbulence. We are focused to find the alternative source of renewable energy; which we can generate the energy in the form of electricity; which should be more reliable, non-toxic, pollution free in nature, etc. for the purpose of generating power the "sun" can be the best source by making a photovoltaic cell with appropriate absorbing layer which can absorb the sun rays in a huge amount and gives the maximum conversion into electricity. The device which is used for the conversion of sun rays into electricity called photovoltaic devices and these devices are based on the principle of photoelectric effect. Moreover, in the universe at a very large volume there is waste heat energy to recover. For the purpose of converting the sun rays into

the usable electrical energy, only the photovoltaic materials can be the promising materials and the instrument which we are using for this convergence of sun rays into the electrical energy is called photovoltaic cells; which is the alternative and the long-time resource of power generation. Also, these power generators are eco-friendly in nature which is very good for our climate and they are having outstanding advantages as compare to other conversion devices [1]. There are numerous of materials are studied for photoelectric devices which are organic substances, Perovskites, Half-Heusler, Anti-Perovskites, Double-Perovskites, Chalcogenides, etc. [2]. In this research work, we are investigating the chalcopyrite crystal structured solids. These crystals having general formula $A^{I}B^{III}X_2^{VI}$. These compounds having many applications likewise in photovoltaic devices, linear and non-linear optical devices etc. [3-4], these compounds are low and direct band gap semiconductors ranging from 1eV to 3eV [5-6]. Which are useful in semiconductor as well as in photovoltaic devices. These compounds possess body centred tetragonal symmetry with I42d space group [7-8]. These compounds are stable, more efficient and can be the alternative for the absorbing layer in thin film solar cell technology or in the photovoltaic devices [9]. Plirdpring *et al.* [10] have reported that the chalcopyrite structured solids can be the promising material for the thermoelectric generator (TEG) also they are good and useful substance in the high-temperature applications. Ranjan *et al.* [11] have investigated $AgTiX_2$ chalcopyrite compound and they found that this compound can be the promising material for the optoelectronic and the photovoltaic applications in the solar cells. Also, it has been reported that the tetragonal structured chalcopyrites possess large Gruneisen parameters and the low phonon group velocities it means the lattice thermal conductivity is lower for these compounds which are useful in the solar cells [12]. Moreover, the 'Sb'-based chalcopyrites are also started investigated for optical and thermal properties [13-14]. According to the study of numerous research articles we can conclude that in the contribution of making absorbing layer in solar cells chalcopyrite materials can be the potential candidate also we can say that the photoelectric devices can be the alternative resource for the production of renewable and green energy. Only those compounds are favourable for thermoelectric devices which possess less thermal conductivity and high-power factor [15]. So, in this research work we are investigating the body centred tetragonal crystal structured chalcopyrite compounds $LiGaX_2$ (X=S, Se). We are calculating the structural, electronic, mechanical and optical properties for these couple of chalcopyrite crystal structured compounds by using the density functional theory (DFT) implemented in the WIEN2k and ATK-VNL simulation code. These kinds of compounds are also investigated for the storage devices; but here we are doing calculation to find a chalcopyrite compound that can be used in the photovoltaic devices which should be worth it, non-toxic, reliable, cheaper in cost, more efficient, stable and pollution-free. The efficiency of chalcopyrite based thin film solar cells exceeds from 23.4% [16-17]. A theoretical study is important for taking the benefits of these couple of chalcopyrite composites $LiGaX_2$ (X=S, Se) for the application in photovoltaic devices. The construction of this research paper is as follows: In section 2. Methodology and computational details, in section 3. Results and discussion and in section 4. Summary and conclusion.

I. Computational details

For this study there was mainly four steps performed: (a) For the calculations of lattice parameters of the crystal structure and volume optimization (structural properties), (b) For the calculation of electronic parameters of the material i.e., band-structure and the density of states (electronic properties), (c) For determination of dielectric constant and the calculation of optical parameters (optical properties)and (d) For the calculation of elastic properties of the tetragonal crystal structured chalcopyrite compounds i.e., $LiGaX_2$ (X=S, Se).For the calculation of above-mentioned properties, we have used the DFT model (Density Functional Theory) [18-19] which is implemented in the ATK-VNL (Atomistic Tool Kit – Virtual Nano Lab) and WIEN2k simulation code. For these calculations we have used two simulation codes one is the ATK-VNL code [20] and another one is WIEN2k code [21] whereas, the WIEN2k is based on the full potential linearized augmented plane wave (FP-LAPW) [22] and the ATK-VNL is based on the pseudo potential plane wave. For understanding the structural parameters, band structure and band-gap of the compounds $LiGaS_2$ and $LiGaSe_2$ we have used the both simulation codes. For studying the elastic parameters, we have used ATK, for determining the optical properties we have used WIEN2k code. For the investigation of structural, electronic and elastic properties by ATK-VNL simulation code, we have been used the double zeta polarized basis sets, LDA and GGA exchange correlation potentials and the crystal structure were optimized until each and every atom of the crystal body attains the force convergence criteria and the maximum stress i.e., 0.05 eV/Å^3, for this optimization process there was 200 steps were performed and the step size was 0.2Å which is by default fixed into the simulation code. We used the 24*24*24 k-mesh [23] and removed the constrain in x, y and z directions. For the ground state energy convergence, we have set it at 150 Ryd. because we can obtain the convergence at ground state only when we apply the mesh-cut-off energy from various convergence test it was found that the 150 Ryd. is most favourable value for the accuracy of our calculations. Also, for studying the electronic parameters we have used PBE-GGA [24], WC-GGA [25-26], LDA [27] and PBEsol-GGA [28] exchange-correlation potential whereas for studying the structural and optical parameters we have used the PBE-GGA exchange-correlation potential in the WIEN2k code, for these calculations Monkhorst-Pack k-point sampling 21×21×21 have been used. The cut off parameters control the size of basis sets so the value of $R_{mt}K_{max}$ is set to 7 for all studied system. where R_{mt} stands for the smallest radius of muffin-tin sphere and K_{max} stands for the magnitude of the largest K vector in the plane wave expansion. The value of $l_{max} = 10$ also potential and the charge density were expanded up to $G_{max} = 10$. The R_{mt}(muffin tin radii)of Li, Ga, S and Se are

tabulated in table 1.The condition of convergence for energy and the charge disparity in successive iterations of SCF cycles have been fixed i.e., 0.00001 Ry and 0.0001e respectively. To investigating optical parameters of our compounds we have used the dense k-mesh 21×21×21. These calculations are done without spin consideration by both simulation codes. Moreover, to calculate the accurate band-gap we employed the TB-mBJ [29] (modified Trans and Blaha potential) with PBE-GGA exchange correlation potential functional because the optical parameters are depending upon the accuracy of electronic properties so we need the accurate band gap as well as accurate band structure curve.

Table 1

R_{mt} (Muffin tin radii) of $LiGaX_2$ (X=S, Se).

R_{mt} (a.u)	Compounds	
	$LiGaSe_2$	$LiGaS_2$
Li	1.8900	1.8600
Ga	2.2300	2.1600
X	2.2300	1.8600

II. Results and Discussion

2.1. Structural Properties

The lithium atom (Li) resides at (0,0,0); (0, 1/2, 1/4), gallium (Ga) at (1/2, 1/2, 0); (1/2, 0, 1/4) and the X atom at (u, 1/4, 1/8); (-u, 3/4, 1/8); (3/4, u, 7/8); (1/4, -u, 7/8) Wyckoff positions respectively. The unit cell of the compounds $LiGaX_2$ (X=S, Se) are shown in the Fig. 1, these semiconducting materials are crystallizing into the chalcopyrite crystal structure with *122-I42d*space group also the polyhedron for these compounds is tetrahedron. In each unit cell of $LiGaX_2$ (X=S, Se) the lithium (Li) and gallium (Ga) atoms are co-ordinated by four selenium (S, Se) atoms and the selenium (Se), sulphur (S) atom is surrounded by two gallium (Ga) and two lithium (Li) atoms, the co-ordination number for each atom in these unit cells is four (4), these ions form the tetragonal structure. To obtain the accurate lattice constants (a and c in Å), exact location of atoms, bulk modulus (B in GPa) (i.e., the stability of the titled compounds as its volume influenced under the pressure is calculated by bulk modulus), ground state energy and first derivative of bulk modulus (B′) the crystal structure shown in Fig.1 were optimized by using the Murnaghan equation [30] in WIEN2k code [31,32].

$$E(V) = E_0 + \left[\frac{BV}{\mathrm{B}'}\left(\frac{1}{(\mathrm{B}'-1)}\left(\frac{V_0}{V}\right)^{\mathrm{B}'} + 1\right) - \frac{BV_0}{(\mathrm{B}'-1)}\right]$$

$$P(V) = \frac{B}{\mathrm{B}'}\left\{\left(\frac{V_0}{V}\right)^{\mathrm{B}'} - 1\right\},$$

Here, $P = -\frac{dE}{dV}$, $\mathrm{B}' = -\mathrm{V}\frac{dP}{dV} = V\frac{d^2E}{dV^2}$

In the above-mentioned equation of state, E_0 stands for equilibrium energy at 0 kelvin temperature, B stands for the bulk modulus, B′ stands for first derivative of bulk modulus, V stands for volume of the unit cell and V_0 stands for the equilibrium volume at 0 pressure. To calculate the accurate lattice parameters there are "six" values were given for each volume then a polynomial was fixed to the computed energies. The plot of total energy as a function of volume for these chalcopyrite materials are shown in the Fig. 2 and the calculated lattice constants (a=b and c), bulk modulus (B), first derivative of bulk modulus (B′), equilibrium volume (V_0), equilibrium energy (E_0)is tabulated in table. 2. The calculated lattice constants of titled compounds lies in between the range "a=b =5.287 to 5.826 Å" "c =10.114 to 11.255 Å" which are having the good agreement with the previous research studies. The thermoplastic properties are expressed by first derivative of bulk modulus and from our calculation, we conclude that it is positive for both chalcopyrites it means with the increment in pressure these compounds will be stiffer which is good for their use in solar devices. Also, from our study we conclude that these compounds possess the most stable geometry in the tetragonal symmetry.

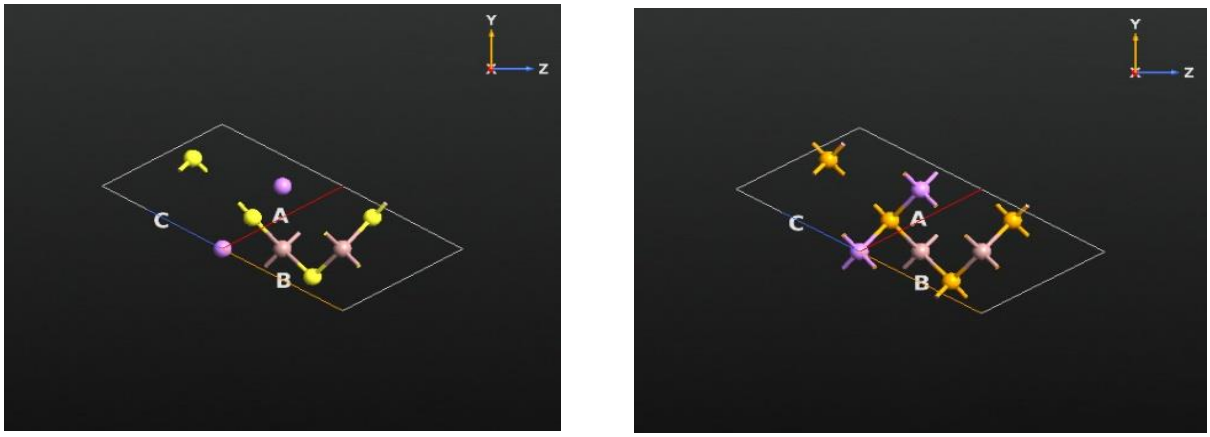

(a) $LiGaS_2$ (ATK-VNL) **(b) $LiGaSe_2$ (ATK-VNL)**

Fig. 1. (a, b) crystal structure obtained by ATK-VNL and WIEN2k. In Fig. 1. (a) Purple color represents Li-atom, brown color represents Ga-atom and yellow color represents S-atom of $LiGaS_2$ compound and in the Fig.1. (b) Purple color represents Li-atom, brown color represents Ga-atom and gold color represents Se-atom of $LiGaSe_2$ compound.

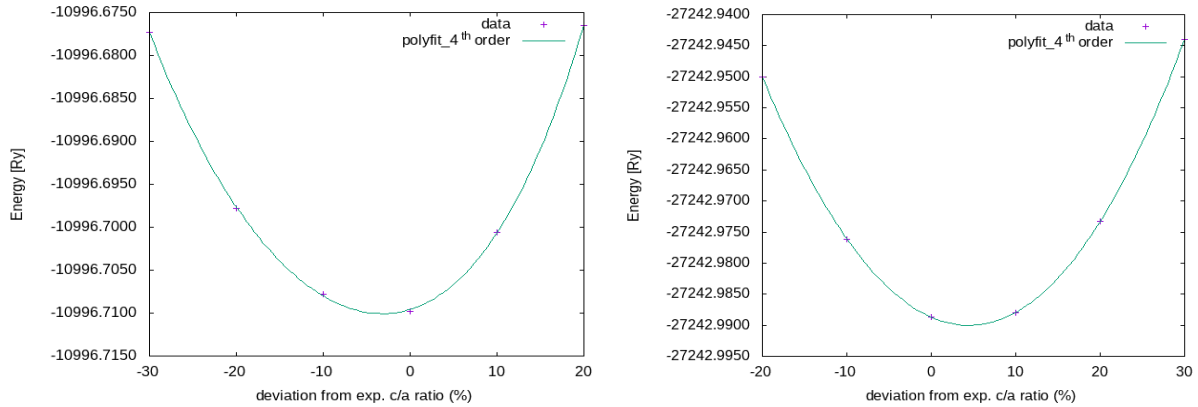

(a) $LiGaS_2$ **(b) $LiGaSe_2$**

Fig. 2. (a and b) Calculated total energy vs lattice constants of $LiGaX_2$ (X=S, Se).

Table 2

Structural Parameters: - Lattice constants (a=b and c), Bulk Modulus (B), Derivative of Bulk Modulus (B′), Equilibrium Volume (V_0) and Energy (E_0) of $LiGaX_2$ (X=S, Se).

Compounds	Lattice Constants (Å)				B(Gpa)	B′	V_0	E_0
	WIEN2k		ATK					
	a=b	c	a=b	C				
$LiGaSe_2$	5.826	11.255	5.754	10.295	52.09	4.617	1167.4276	-27212.169
$LiGaS_2$	5.287	10.114	5.333	10.445	52.66	4.037	1077.8304	-11000.748

2.2. Electronic properties

2.2.1. Electronic Bandgap and Band Structure Curve

In this study, electronic band-structure and the band-gap of $LiGaX_2$ (X=S, Se) ternary chalcopyrite have been calculated by two simulation codes without considering the spin-orbit coupling which are explained in section. 2, there was two exchange correlation potentials used in ATK i.e., LDA and GGA and four exchange correlation potentials used in WIEN2k i.e., LDA, WC, PBE and PBEsol to run the scf cycle by using the lattice constants which are obtained by the optimization of the structure, the band-structures are depicted in Fig.3 and the calculated electronic band-gaps compared with experimental band-gaps are tabulated in table. 3 if we are comparing the experimentally predicted bandgaps with calculated bandgap of these compounds the calculated bandgap don't have good consistency with existing information. So, we need to calculate more accurate bandgaps for the chosen compounds. Hence, for this purpose we apply the TB-mBJ (modified Trans and Blaha potential) method with PBE-GGA exchange correlation potential functional. By applying this method, we get the bandgaps with good consistency with experimentally obtained data. Also, from this table we conclude that the band gap is decreasing when we move from "S" atom to "Se" atom which confirms the theoretical perception of bandgap variation phenomena. The accuracy of optical properties is based on the electronic properties (band structure) so firstly described the band structure then explained the optical properties. The plots in the Fig. 3 are plotted in between the energy function and the wave vector denoted by 'K' for the chosen compounds in the first Brillion Zone, these plots are band structure curves. The band-structure curve basically displays the band-gap of the compounds from which we can confirm that the compounds are semiconductor material or not. From the calculated band structure curve, we can see that our compounds namely $LiGaX_2$ (X= S, Se) possess direct band gap and their directivity lies on Γ-Γ. The calculated energy to separate low and high energy states are -0.24590 eV, -0.30567eV and the Fermi energy achieved 0.23676 eV, 0.14832eV for $LiGaX_2$ (X= S, Se).

2.2.2. Density of states

For the better understanding about electronic properties i.e., the complete study of the interaction between the numerous orbitals of atoms, we calculated the density of states of the titled compounds by using the TB-mBJ method with PBE-GGA exchange correlation potential which are shown in Fig. 4. For both the compounds fermi-level have been fixed at 0 eV. We measured the partial density of states for the exact study of hybridization. From our study we conclude that the density of states of the mentioned compounds share the same features. For the detailed information we distorted TDOS (total density of states) into the parts of s, p, d and f orbitals. Fig. 4 (a and e) represents the TDOS of $LiGaS_2/Se_2$, Li, Ga and S/Se and we can see that the major contribution is in the valence band of the atoms as compare to the conduction band. Moreover, the sulphur (S) and selenium (Se) atom contributes the most as compare to the gallium (Ga) and lithium (Li) atom. From Fig. 4 (b and f) we can say that the lithium (Li) atom in both compounds show negligible contribution in valence as well as conduction band with d-state, from Fig. 4 (c) we observe that we get the major peak of gallium (Ga) atom with s-state in conduction band from the range 4.2 eV to 6 eV energy interval also just lower than this peak we get

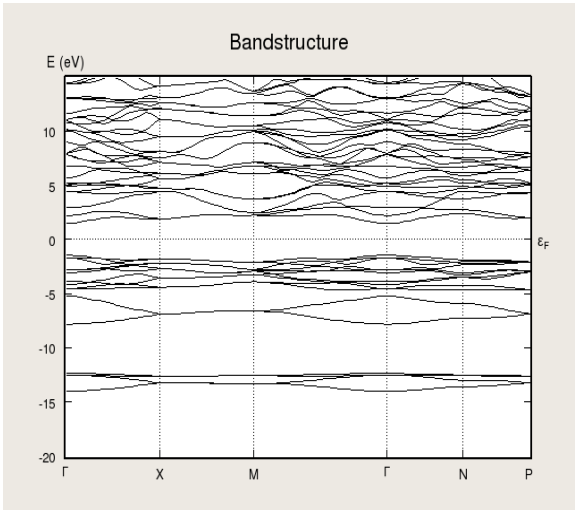

(a) $LiGaS_2$ (ATK-VNL)

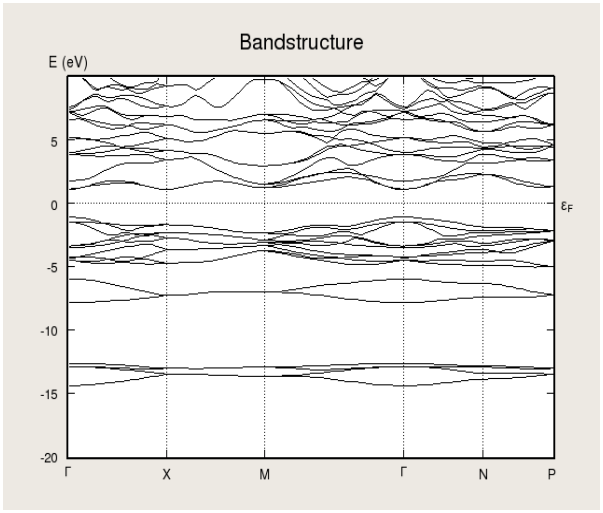

(b) $LiGaSe_2$ (ATK-VNL)

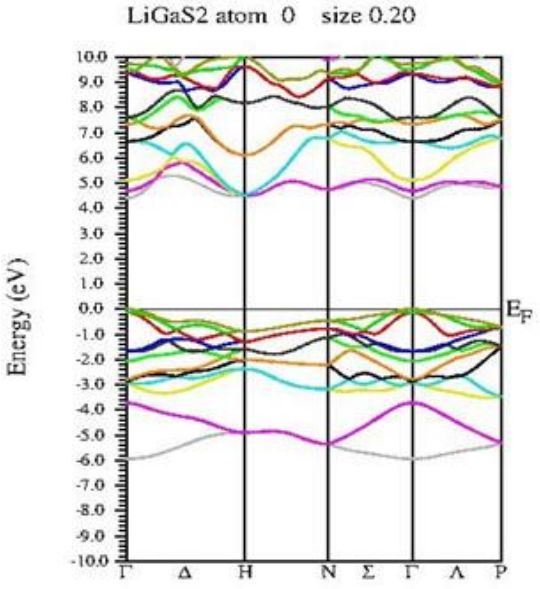

(c) $LiGaS_2$ (WIEN2k)

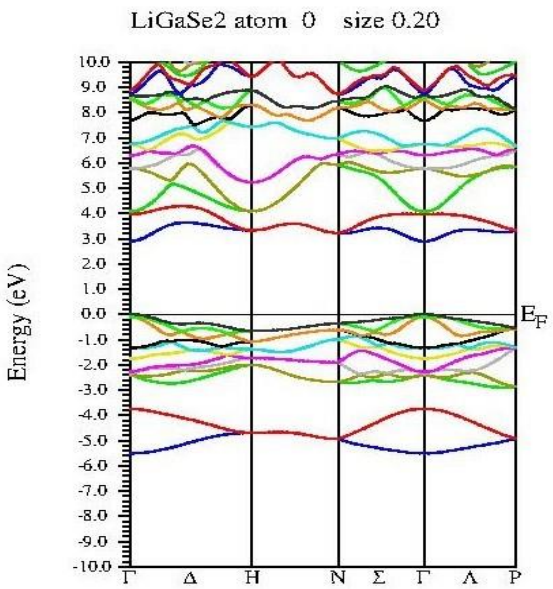

(d) $LiGaSe_2$ (WIEN2k)

Fig. 3. (a, b, c, d) Calculated band-structure-curves of $LiGaX_2$ (X=S, Se) by ATK-VNL and WIEN2k.

Table 3

Electronic-band-gaps of $LiGaX_2$ (X=S, Se).

Compounds	Band-Gap (eV)							
	ATK		WIEN2k					Experimental
	LDA	GGA	LDA	WC	PBE	PBEsol	TB-mBJ	
$LiGaSe_2$	2.578	2.178	1.671	1.746	1.863	1.777	2.903	3.13[a]
$LiGaS_2$	2.757	2.919	3.056	3.068	3.277	3.094	4.415	4.15[a]

[a]Ref [42]

the 2nd peak of gallium (Ga) atom with s-state in the valence band from the range -6 eV to -5 eV energy interval, we get the major peaks of gallium (Ga) atom with p-state in valence band from the range -4.2 eV to 0 eV energy interval and lower peaks in the conduction band with p-state in the range of 4.3 eV to 7 eV energy interval, negligible contribution with d-state and f-state of gallium atom (Ga) shown in the valence as well as in the conduction band, so the gallium atom (Ga) shows the sp-hybridization in both bands. In the Fig. 4 (d and h) sulphur (S) and selenium (Se) atom shows some peaks in the conduction band with d-state they contribute in the conduction band only with d-state. From Fig. 4 (g) we can say that we get the major peak of gallium (Ga) atom with s-state in the valence band from range -6.3 eV to -4.1 eV energy interval and in the conduction band from range 2.5 eV to 4.1 eV energy interval with the s-state, we get the major peaks of gallium atom (Ga) with p-state in the conduction band from range 2.6 eV to 7eVenergy interval than get peaks in the valence band of gallium atom (Ga) with p-state from range -4.5 eV to 0 eV energy interval from this it is clear the contribution of gallium atom (Ga) in both bands is due to the sp-hybridization because the p and d-states of the gallium atom (Ga) shows the negligible contribution in both the bands. So, mainly the contribution is due to the sp-hybridization in both the above-mentioned

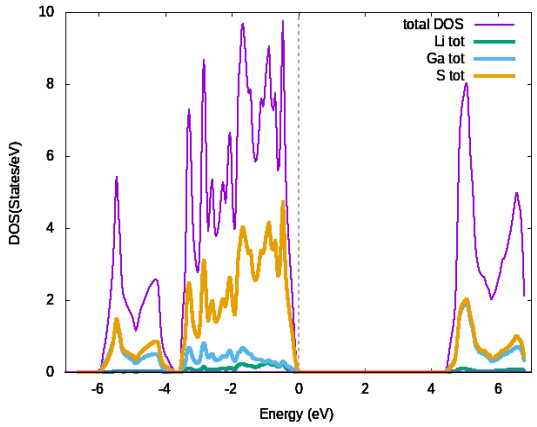

(a). Total DoS of $LiGaS_2$, Li, Ga, S atoms

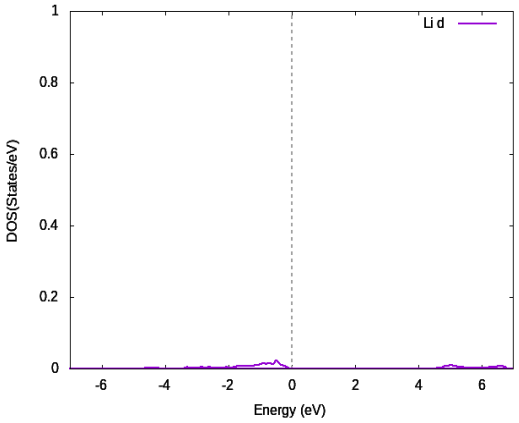

(b). Partial DoS of Li-atom in$LiGaS_2$

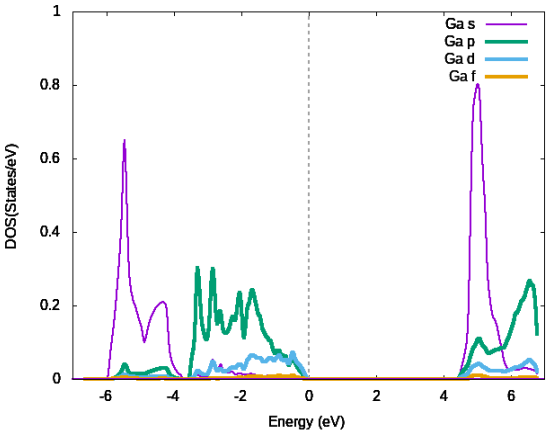

(c). Parial DoS of Ga-atom in $LiGaS_2$

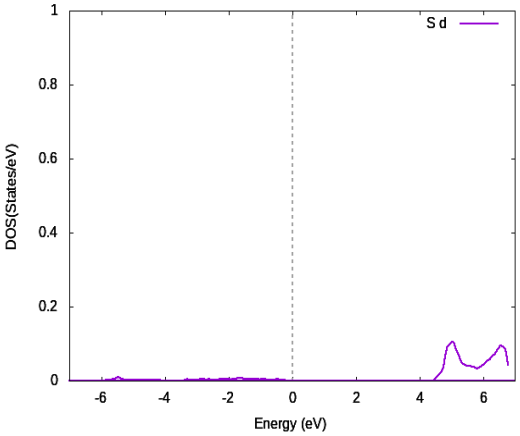

(d). Parial DoS of S-atom in $LiGaS_2$

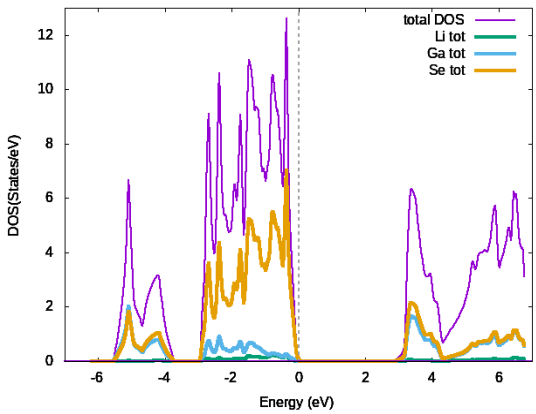

(e). Total DoS of $LiGaSe_2$, Li, Ga, Se atoms

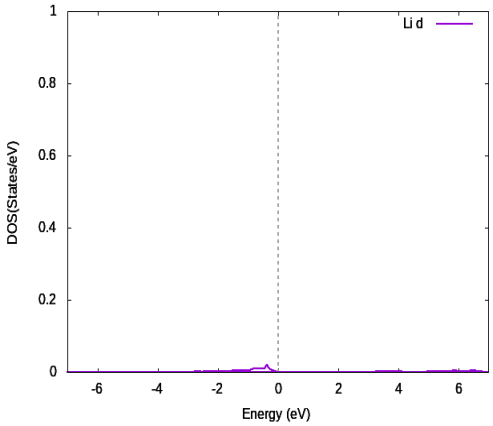

(f). Parial DoS of Li-atom in $LiGaSe_2$

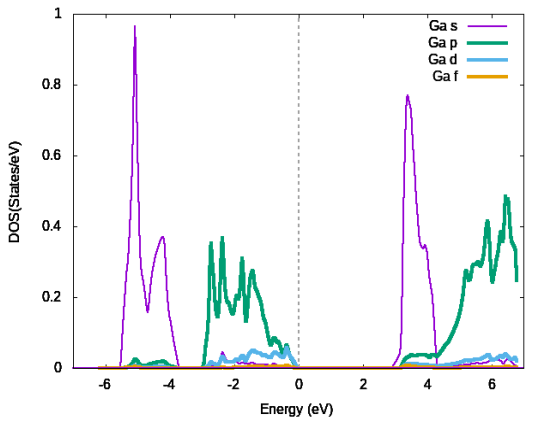

(g). Parial DoS of Ga-atom in $LiGaSe_2$

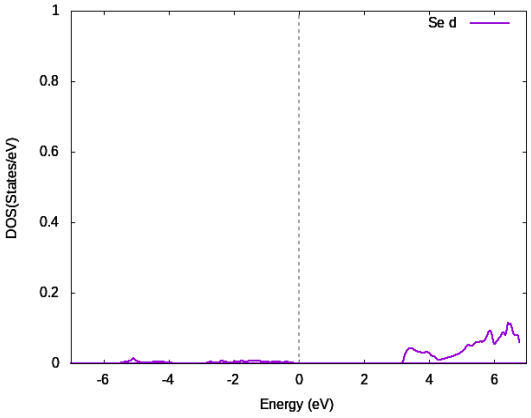

(h). Parial DoS of Se-atom in $LiGaSe_2$

Fig. 4. (a, b, c, d, e, f, g, h) Calculated total and partial density of states (DOS) of $LiGaX_2$ (X=S, Se).

compounds in the valence as well as the conduction band.

2.3. Optical Properties

After optimization of the crystal structure, we get the wave function in the numerical format of the computed electronic states and one of them can be computed by the study of optical properties by computing the dielectric function of the compound. Basically, optical properties of an element define the collaboration with electromagnetic waves i.e., this collaboration defines the optoelectronic applications. For the titled compounds we have been studied the various features likewise the dielectric constant denoted by '$\varepsilon(\omega)$', absorption coefficient denoted by '$\alpha(\omega)$', optical conductivity denoted by '$\sigma(\omega)$', extinction coefficient denoted by '$k(\omega)$', refractive index denoted by '$n(\omega)$', reflectivity denoted by '$R(\omega)$' and the energy loss function denoted by '$E_{loss}(\omega)$'. These optical parameters are depending upon the electronic properties.

The complex dielectric function calculates the linear response to electro-magnetic field for a small wave vector.

$$\varepsilon(\omega) = \varepsilon_1(\omega) + i\varepsilon_2(\omega) \quad (1)$$

Equation (1) called the Ehrenreich and Cohen's equation [33]

Here the 'ω' denotes angular frequency of incident electro-magnetic wave, '$\varepsilon_1(\omega)$' is the real part which defines the polarization of electrons and the irregular distribution in substances, '$\varepsilon_2(\omega)$'is the imaginary part which defines the optical absorption and this imaginary part '$\varepsilon_2(\omega)$'can be stated as: [2]

$$\varepsilon_2(\omega) = \frac{4e^2\pi^2}{\omega^2 m^2}\sum_{i,j}\int |\langle i|M|j\rangle|^2 f_i(1-f_i).\delta\left(E_f - E_i - \hbar\omega\right)d^3k \quad (2)$$

In the above equation (2) [34] the 'ω' represents the angular frequency of incident photon, 'e' represents the charge of the electron, 'm' represents the mass of the electron,'ħ'represents the plank's constant, 'M' represents the momentum operator, whereas 'i' and 'j' stands for valence band which is the initial state and conduction band which is the final state, 'f_i' defines the fermi dispersion function for the initial state, '$\delta\left(E_f - E_i - \hbar\omega\right)$'defines the energy variation among valence and the conduction bands on the k-point which absorbs the incident photon having energy ħω.We can calculate the real part '$\varepsilon_1(\omega)$' from the imaginary part '$\varepsilon_2(\omega)$'by using Kramers-Kronig 's equation [35]:

$$\varepsilon_1(\omega) = 1 + \frac{2}{\pi}P\int_0^\infty \frac{\omega'\varepsilon_2(\omega')}{\omega'^2-\omega^2}d\omega' \quad (3)$$

In the above equation (3), 'P' stands for the principle value of integral, the all remaining optical parameters i.e., absorption coefficient, refractive index, extinction coefficient and spectrum of energy-loss can be evaluated by the '$\varepsilon_1(\omega)$' and '$\varepsilon_2(\omega)$' [36-37]. The calculated optical parameters of the titled compounds in the range from 0 eV to 10 eV are shown in the Fig. 5. (a-h). The Fig. 5. (a and b) shown the real $\varepsilon_1(\omega)$ and imaginary part $\varepsilon_2(\omega)$ of dielectric constants of the compound $LiGaX_2$ (X=S, Se). The major peaks of the real part of dielectric function produced by the transformation of electrons from the top of valence band to the bottom of conduction band and we get these peaks at 5.22 eV for $LiGaS_2$, and 3.3 eV for $LiGaSe_2$ respectively. The $\varepsilon_1(\omega)$ spectrum started decreasing up to 6.23 eV for $LiGaS_2$ and 4.33 eV for $LiGaSe_2$ respectively. By doing computation for these optical parameters, we conclude that these compounds are anisotropic. We observe that when we are moving from 'S' to 'Se' peaks are increasing and then started decreasing toward the lower energy interval in the $\varepsilon_1(\omega)$spectrum i.e., real part of the dielectric function. The fundamental feature of optical spectrum is the imaginary part of the dielectric constant$\varepsilon_2(\omega)$of the material, Fig. 5. (b) shown the imaginary part of dielectric function $\varepsilon_2(\omega)$, in this spectrum we observe the critical points obtained at 4.4 eV for $LiGaS_2$and 2.42 eV for $LiGaSe_2$ respectively, these critical points provide threshold for the traditional optical transformation among the valence and the conduction band so, these points called the fundamental absorption edge, moreover we have noticed that the observed fundamental edges are very close to the calculated band-gaps i.e., 4.415 eV for $LiGaS_2$ and 2.903 eV for $LiGaSe_2$ respectively, Fig. 5. (c) shown the refractive index of $LiGaS_2/Se_2$, this spectrum shows the anisotropic nature of the titled compounds. The Δn for $LiGaS_2/Se_2$ at 0 eV are 0.0136 and 0.0408 respectively. In this work, calculated refractive index for $LiGaS_2/Se_2$ 2.1 and 2.3 respectively, also we analyzed that when the energy approached at the highest point in the visible reason the refractive index increased, and then started decreasing with increasing the energy intervals in both compounds. We get the major peaks 2.97 at 5.56 eV for $LiGaS_2$ and 3.1 at 3.98 eV for $LiGaSe_2$ respectively, also we can observe that when we are moving towards 'S' to 'Se' the peaks are going to lower energies. We have calculated the decay of amplitude oscillation for the incident electro-magnetic radiation by calculating the extinction coefficient $k(\omega)$ which is shown in the Fig. 5. (d) for $LiGaS_2/Se_2$ and we observe that we get the major peaks of extinction coefficient close to the frequencies at the point where $\varepsilon_1(\omega)$ reaches to the value '0'after this it starts decreasing with increasing the photon energy. Fig. 5. (e) shown the reflectivity of $LiGaS_2/Se_2$ we observe that the reflectivity of the titled compounds lies in the ultra-violet region of the electromagnetic spectrum, therefore the chosen compounds may be the reliable compounds armors for UV-rays of high energy as well as reliable for photovoltaic application in visible and IR-regions of electromagnetic spectrum. We calculated the degeneration in the energy for the electron which is revolving into the substance by calculating the we can see energy loss $E_{loss}(\omega)$ which is shown in the Fig. 5 (f) that the perceptible peaks are obtained in the ultra-violet region of EM spectrum i.e., from 3.26 eV to 14.0 eV for the chosen compounds. When the EM wave is passing through a specimen some light is absorbed by its

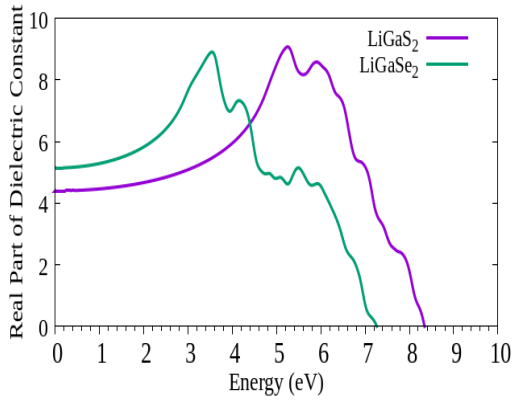

(a). Real Part of Dielectric Constant $\varepsilon_1(\omega)$

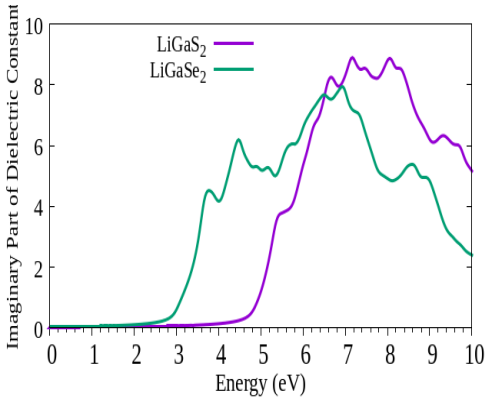

(b). Imaginary Part of Dielectric Constant $\varepsilon_2(\omega)$

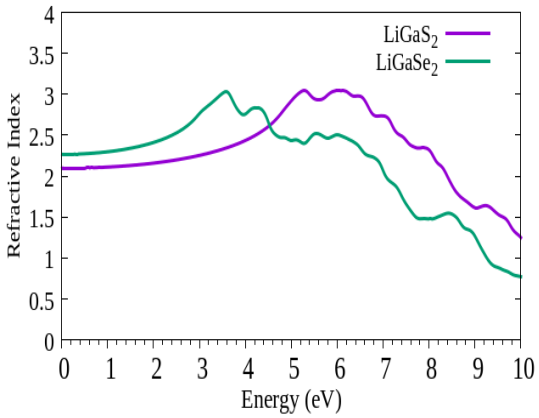

(c). Refractive index $n(\omega)$

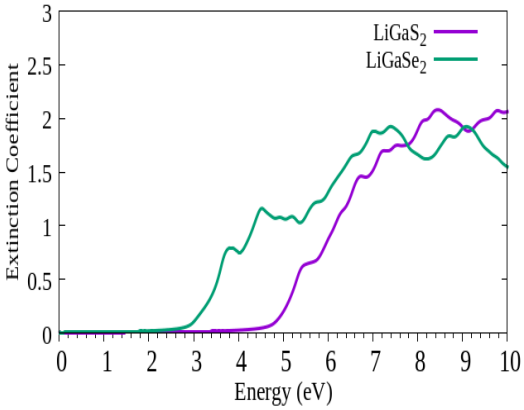

(d). Extinction Coefficient $k(\omega)$

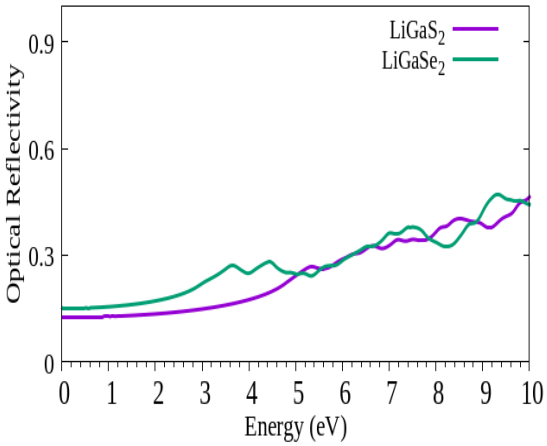

(e). Reflectivity $R(\omega)$

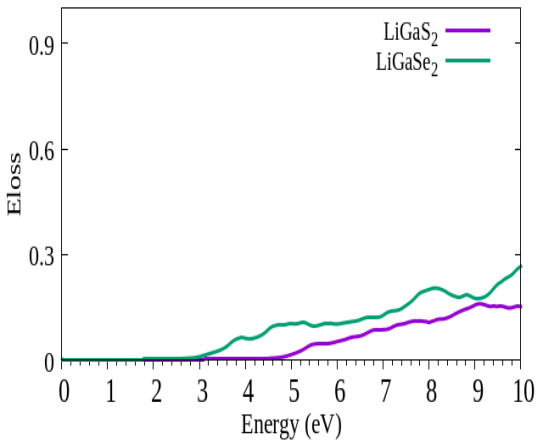

(f). Eloss $E_{loss}(\omega)$

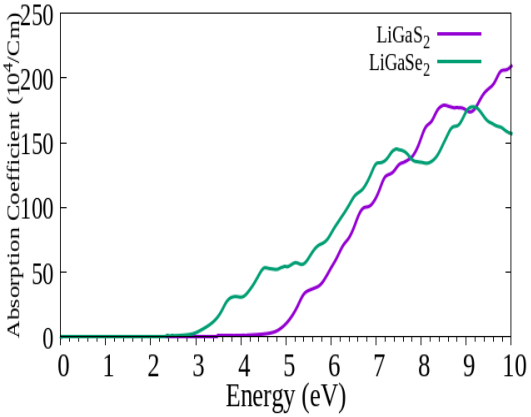

(g). Absorption Coefficient $\alpha(\omega)$

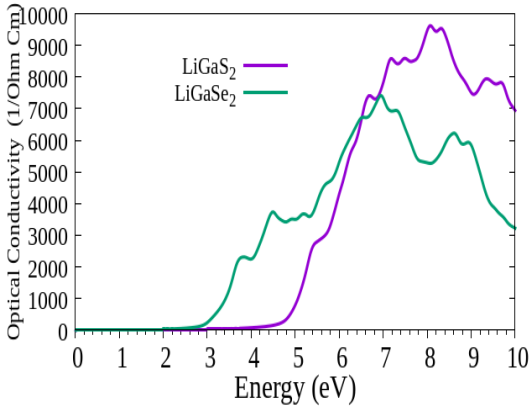

(h). Optical Conductivity $\sigma(\omega)$

Fig. 5. (a, b, c, d, e, f, g and h) Calculated Optical parameters of $LiGaX_2$ (X=S, Se).

unit depth called the absorption coefficient '$\alpha(\omega)$' which is shown in the Fig. 5 (g) we observed that the polarization has been influenced the EM spectrum, we get the absorption edges at 4.9 eV for $LiGaS_2$ and 3.2 eV for $LiGaSe_2$ respectively which is the UV-region it means the chosen compounds' s absorbance lies in the UV-range, if photon energy is greater than absorption value then the absorption coefficient will be increased. We can see that the absorption coefficient decreases when the photon energy increases i.e., this is the traditional feature of semiconductors. We calculated the optical conductivity for the titled compounds which is shown in the Fig. 5 (h) the optical conductivity is used to calculate the efficiency of conversion phenomena of photon energy into the electric energy. We observe that the chosen compounds' s optical conductivity lies in the UV-region ranging from 3.1 eV to 4.4 eV. So, these compounds can be worth it for the photovoltaic cells.

2.4. Elastic Properties

Elastic property is the most important feature of solids and it can be measured by using the first principle approach. As we know that the titled compounds possess the tetragonal configuration so the tetragonal crystal structure's elasticity predicted by the six elastic constants C_{ij} i.e., C_{11}, C_{12}, C_{13}, C_{33}, C_{44} and C_{66}. These constants provide us the most significant info regarding the stability of the crystal structure, anisotropy of solid crystals, mechanical properties, bond-index of the solids etc. There are some necessary conditions called Born-Huang conditions [38] which are most required to fulfil by the solid crystal structures.

The necessary conditions for the tetragonal solids are as follows:

$$C_{11} > 0,\ C_{33} > 0,\ C_{44} > 0,\ C_{66} > 0,$$

$$(C_{11} - C_{12}) > 0,\ (C_{11} + C_{33} - 2C_{13}) > 0,$$

$$\{2(C_{11} + C_{12}) + C_{33} + 4C_{13}\} > 0.$$

For determining the above C_{ij} elastic constants we need mainly the five equations, the first one consists B (Bulk Modulus), the equation in the form of the elastic constants is as follows:

$$B = \frac{(C_{11}+C_{12})C_{33} - 2C_{13}^2}{C_{11} + C_{12} + 2C_{33} + 4C_{13}^2}$$

Also, the zener anisotropy factor is the most significant feature of elastic properties and it is represented by 'A', if we get the value of A then we determine the stability of the solids or crystals. If we get A is equal to one the solid or compound is isotropic, if we get A less than or greater than one the solid is anisotropic, the compounds whose features are depend on direction known as anisotropic compounds.

Zener anisotropic factor in the terms of elastic constants C_{ij} is as follows:

$$A = \frac{C_{44}}{C_{11-C_{12}}}$$

For the applications which are calculated by using the mentioned relations [39]:

The young's modulus represented with the symbol 'Y', it is generally used for determining the stiffness of the solids, in the terms of B and G the young modulus is written below:

$$Y = \frac{9GB}{G+3B}$$

The poisson's ratio represented with the symbol 'υ', the numerical value of this ratio generally observed in the range from 0 to 0.5 for the numerous compounds, also this ratio provides us the info related to the characteristics of the binding forces acting in the compounds. If central force is acting between the atoms of compound it's range from 0.25 to 0.5 respectively.

In the terms of B and G the poisson's ratio is written below:

$$\upsilon = \frac{1}{2}\left[\frac{B-2/3\ G}{B+1/3\ G}\right]$$

Now, the anisotropic shear modulus(G):

$$G = \frac{G_V+G_R}{2}$$

The constant G_v represents the voigt's shear modulus corresponding to the upper bound values of the shear modulus G,

and the constant G_R represents the reuss's shear modulus corresponding to the lower bound values of the shear modulus G.

$$G_v = 1/30\ (4C_{11} + 2C_{33} - 4C_{13} - 2C_{12} + 12C_{44} + 6C_{66})$$

$$G_R = 15\ [(18B_V/C^2) + [6/\ (C_{11} - C_{12})] + (6/C_{44}) + (3/C_{66})]^{-1}$$

$$B_v = (1/9)\ [2(C_{11} + C_{12}) + C_{33} + 4C_{13}]$$

$$C^2 = (C_{11} + C_{12})C_{33} - 2(C_{13})^2$$

Here in the above-mentioned values in the terms of the constants, the subscript 'V' represents the voigt bound and the 'R' represents the reuss bound [40]. In this work we also calculated the Pugh's ratio which is basically denoted by the B/G here B is the bulk modulus and G is the shear modulus it is calculated because by getting the numerical value of pugh's ratio we can confirm that our compound is ductile or brittle in nature. The compound is brittle or ductile this feature is only decided by this ratio. The pugh's ratio is the simplest relation which shows the behaviour of the material weather it is ductile or brittle in nature [41]. If we get the value of B/G less than 1.75 the material is brittle in nature and if we get B/G's value more than 1.75 the material is ductile in nature. By using the above-mentioned formulas of modulus of elasticity we can easily calculate the mechanical features of the solid crystal structures. Also, by using the approach namely Voigt-Reuss-Hill averaging approach [42]. The measured elastic constants C_{ij} are tabulated in table. 4, the properties of compounds measured by using elastic constants in GPa are tabulated in table. 5, 5.1 and 5.2, the measured zener anisotropy factor 'A' and B/G ratio are tabulated in table 6. These measurements proves that our chosen compounds $LiGaX_2$ (X= S, Se) are the mechanically stable compounds.

Table. 4

We calculated the elastic constants C_{ij} for $LiGaX_2$ (X = S and Se) by applying the ATK-VNL with GGA-PBE exchange correlation potential which are tabulated below:

Compound	Elastic constants in GPa					
	C_{11}	C_{12}	C_{13}	C_{33}	C_{44}	C_{66}
$LiGaS_2$	55.92	56.04	50.85	32.75	33.21	24.07
$LiGaSe_2$	84.80	84.87	76.11	36.80	37.06	23.08

Table. 5

The calculated material properties using elastic constants in GPa are tabulated below:

5.1. for $LiGaS_2$:

	Reuss	Voigt	Hill
Bulk modulus:	36.67	38.86	36.77
Shear modulus:	17.94	23.22	20.58
	X	**Y**	**Z**
Young's modulus:	35.7539	35.9264	20.0770
	XY	**XZ**	**YZ**
Poisson's ratio:	0.0107	0.4195	0.4169
	YX	**ZX**	**ZY**
	0.0107	0.4230	0.4220

5.2. for $LiGaSe_2$:

	Reuss	Voigt	Hill
Bulk modulus:	58.6753	58.7055	58.6904
Shear modulus:	22.3625	26.3546	24.3586
	X	**Y**	**Z**
Young's modulus:	50.1719	50.3246	34.5888
	XY	**XZ**	**YZ**
Poisson's ratio:	0.1118	0.4095	0.4073
	YX	**ZX**	**ZY**
	0.1114	0.4940	0.4926

Table. 6

We calculated the zener anisotropy factor (A) and the Pugh's ratio (B / G) of $LiGaX_2$ (X = S and Se) which are tabulated below:

Compound	A	B / G
$LiGaS_2$	-276.75	2.04
$LiGaSe_2$	-529.42	2.62

Summary and Conclusion

For the conclusion, the calculated results have represented for the structural, electronic, optical and the mechanical parameters of the body centred tetragonal $LiGaX_2$ (X=S, Se) chalcopyrite structured solids with the help of using the first principle computation, the titled compounds possess direct band-gap, the electronic properties are compared with available experimental data which is calculated by implementing the mBJ-potential and found that good agreement with each other. The calculated optical parameters proves that these compounds are trustworthy for the photovoltaic applications. We calculated the mechanical parameters likewise elastic constants C_{ij}, modulus of elasticity i.e., Young's modulus, Bulk modulus, Shear modulus and Poisson's ratio respectively. The elastic constants are not yet calculated experimentally. From the study of B/G ratio of our material proves that these are ductile materials. The calculated mechanical parameters proves that these materials are mechanically stable materials. The study of optical and elastic properties confirms that these compounds are anisotropic in nature. This study would more inspire the research studies in appropriate field.

Conflict of Interest:

This manuscript does not include conflict of interest.

Jyoti Kumari – master of science, Research Scholar Department of Physics;
Chandravir Singh – Ph.D., Professor Department of Physics;
Banwari Lal Choudhary – Ph.D., Professor Department of Physics;
Ajay Singh Verma – Ph.D., Professor: Division of Research & Innovation.

[1] S. Twaha, J. Zhu, Y. Yan, & B. Li, *A comprehensive review of thermoelectric technology: Materials, applications, modelling and performance improvement*, Renewable and Sustainable Energy Reviews, 65, 698 (2016); http://dx.doi.org/10.1016/j.rser.2016.07.034.

[2] U. Rani, P. K. Kamlesh, R. Agarwal, J. Kumari, & A. S. Verma, *Electronic and thermo-physical properties of double antiperovskites X_6SOA_2 (X= Na, K and A= Cl, Br, I): A non-toxic and efficient energy storage materials*, International J. Quantum Chemistry, 121, 19 (2021); https://doi: e26759 doi:10.1002/qua.26759.

[3] M. S. Khan, T. Alshahrani, B. U. Haq, S. Khan, G. Alrobei, H.& M. Benaadad, *Investigation of structural, electronic and optical properties of potassium and lithium based ternary Selenoindate: Using first principles approach*, J. Solid-State Chemistry, 293, 121778 (2021); https://doi: 10.1016/j.jssc.2020.121778.

[4] M. Ye, R. Tang, S. Ma, Q. Tao, X. Wang, Y. Li, & P. Zhu, *Electrical Transport Properties and Band Structure of $CuInSe_2$ under High Pressure*, J. Physical Chemistry, 123, 20757 (2019); https://doi.org/10.1021/acs.jpcc.9b05499.

[5] L. Yu, A. Zunger, *Identification of potential photovoltaic absorbers based on first-principles spectroscopic screening of materials*, Phys. Rev. Lett, 108, 068701 (2012); https://doi: 10.1103/PhysRevLett.108.068701.

[6] H. Xiao, J. Tahir-Kheli, W.A. Goddar, *Accurate band gaps for semiconductors from density functional theory*, J. Phys. Chem. Lett, 2, 212 (2011); https://doi.org/10.1021/jz101565j.

[7] Y. Li, Y. Liu, J. Chen, C. Zhao, & W. Cui, *Comparison study of crystal and electronic structures for chalcopyrite ($CuFeS_2$) and pyrite (FeS_2)*, Physicochemical Problems of Mineral Processing, 57, (2021); https:// doi: 10.37190/ppmp/129572.

[8] M. S. Omar, *Lattice thermal expansion for normal tetrahedral compound semiconductors*, Materials research bulletin, 42, 319 (2007); https://doi: 10.1016/j.materresbull.2006.05.031.

[9] S. Sharma, A. S. Verma, R. Bhandari, & V. K. Jindal, *Ab initio studies of structural, elastic and thermal properties of copper indium dichalcogenides ($CuInX_2$: X= S, Se, Te)*, Computational materials science, 86, 108 (2014); http://dx.doi.org/10.1016/j.commatsci.2014.01.021.

[10] T. Plirdpring, K. Kurosaki, A. Kosuga, T. Day, S. Firdosy, V. Ravi and S.Y. Amanaka, *Chalcopyrite $CuGaTe_2$: a high-efficiency bulk thermoelectric material*, Advanced Materials, 24, 3622 (2012); https:// doi: 10.1002/adma.201200732.

[11] P. Ranjan, P. Kumar, P. K. Surolia, & T. Chakraborty, *Structure, electronic and optical properties of chalcopyrite semiconductor $AgTiX_2$ (X= S, Se, Te): A density functional theory study*, Thin Solid Films, 717, 138469 (2021); https://doi.org/10.1016/j.tsf.2020.138469.

[12] M. Mukherjee, G. Yumnam, A. K. Singh, *High Thermoelectric Figure of Merit via Tunable Valley Convergence Coupled Low Thermal Conductivity in $A^{II}B^{IV}C_2^{V}$ Chalcopyrites*, J. Phys. Chem, 122, 29150 (2018); https://doi.org/10.1021/acs.jpcc.8b10564.

[13] A. Nomura, S. Choi, M. Ishimaru, A. Kosuga, T. Chasapis, S. Ohno, G. J. Snyder, Y. Ohishi, H. Muta, S. Yamanaka, K. Kurosaki, *Chalcopyrite $ZnSnSb_2$: A Promising Thermoelectric Material*, ACS Appl. Mater. Interfaces, 10, 43682 (2018); https://doi.org/10.1021/acsami.8b16717.

[14] H. Liu, B. Zhao, Y. Yu, Z. He, J. Xiao, W. Huang, S. Zhu, B. Chen, L. Xie, *Theoretical investigations on elastic, thermal and lattice dynamic properties of chalcopyrite $ZnSnX_2$ (X = P, As, Sb) under pressure and temperature: The first-principles calculation*, Int. J. Mod. Phys, 32, 1850329 (2018); https://doi.org/10.1142/S0217979218503290.

[15] J. Liu, Y. Zhao, Z. Dai, J. Ni, & S. Meng, *Low thermal conductivity and good thermoelectric performance in mercury chalcogenides*, Computational Materials Science, 185, 109960 (2020); https://doi.org/10.1016/j.commatsci.2020.109960.

[16] A. Sharan, F. P. Sabino, A. Janotti, N. Gaillard, T. Ogitsu, & J. B. Varley, *Assessing the roles of Cu-and Ag-deficient layers in chalcopyrite-based solar cells through first principles calculations*, J. Applied Physics, 127, 065303 (2020); https://doi.org/10.1063/1.5140736.

[17] G. Regmi, Ashok, A. Chawla, P. Semalti, P. Velumani, S. Sharma, S. N. & H. Castaneda, *Perspectives of chalcopyrite-based CIGSe thin-film solar cell: a review*, J. Materials Science: Materials in Electronics, 31, 7286 (2020); https://doi.org/10.1007/s10854-020-03338-2.

[18] Y. J. Lee, M. Brandbyge, J. Puska, J. Taylor, K. Stokbro, & R. M. Nieminen, *Electron transport through monovalent atomic wires*, Phys. Rev, 69, 125409 (2004); https://doi.org/10.1103/PhysRevB.69.125409.

[19] K. Schwarz, *DFT calculations of solids with LAPW and WIEN2k*, J. Solid-State Chemistry, 176, 319 (2003); https://doi: 10.1016/S0022-4596(03)00213-5.

[20] Atomistic Tool Kit – Virtual Nano Lab (ATK-VNL), Quantum Wise Simulator, Version. 2014.3, http://quantumwise.com/.

[21] P. Blaha, K. Schwarz, G. K. Madsen, D. Kvasnicka, J. Luitz, R. Laskowski, F. Tran, L. D. Marks, Wien2k: An augmented plane wave plus local orbitals program for calculating crystal properties (revised edition), Vienna University of Technology, Austria. (2018)

[22] E. Wimmer, H. Krakauer, M. Weinert, & A. J. Freeman, *Full-potential self-consistent linearized-augmented-plane-wave method for calculating the electronic structure of molecules and surfaces: O_2molecule*, Phys. Rev. Letter, 24, 864 (1981); https://doi.org/10.1103/PhysRevB.24.864.

[23] H. J. Monkhorst, & J. D. Pack, *Special points for Brillouin-zone integrations*, Phys. Rev. Letter, 13, 5188 (1976); https://doi.org/10.1103/PhysRevB.13.5188.

[24] J.P. Perdew, K. Burke, M. Ernzerhof, *Generalized gradient approximation made simple*, Phys. Rev. Letter, 77, 3865 (1996); https://doi.org/10.1103/PhysRevLett.77.3865.
[25] Z. Wu, & R. E. Cohen, *More accurate generalized gradient approximation for solids*, Phys. Rev. B, 73, 235116 (2006) https://doi.org/10.1103/PhysRevB.73.235116.
[26] F. Tran, R. Laskowski, P. Blaha, & K. Schwarz, *Performance on molecules, surfaces, and solids of the Wu-Cohen GGA exchange-correlation energy functional*, Phys. Rev. B, 75, 115131 (2007); https://doi.org/10.1103/PhysRevB.75.115131.
[27] W. Kohn, & L. J. Sham, *Self-consistent equations including exchange and correlation effects*, Physical review, 140, A1133 (1965); https://doi.org/10.1103/PhysRev. 140.A1133.
[28] J. P. Perdew, A. Ruzsinszky, G. I. Csonka, O. A. Vydrov, G. E. Scuseria, L. A. Constantin, K. Burke, *Restoring the density-gradient expansion for exchange in solids and surfaces*, Physical review letters, 100, 136406 (2008); https://doi.org/10.1103/PhysRevLett.100.136406.
[29] F. Tran and P. Blaha, *Accurate band gaps of semiconductors and insulators with a semilocal exchange-correlation potential*, Phys. Rev. Letter, 102, 226401 (2009 https://doi.org/10.1103/PhysRevLett.102.226401.
[30] F. D. Murnaghan, *Differential and integral calculus*, Proc. Natl. Acad. Sci. USA, 30, 244 (1947) https://dx.doi.org/10.1073%2Fpnas.30.9.247.
[31] F. Birch, *Finite elastic strain of cubic crystals*, Physical review, 71, 809 (1947); https://doi.org/10.1103/PhysRev.71.809.
[32] F. D. Murnaghan, *The compressibility of media under extreme pressures*, Proc. Natl. Acad. Sci. USA, 30, 244 (1944); https://dx.doi.org/10.1073%2Fpnas.30.9.244.
[33] T. Lantri, S. Bentata, B. Bouadjemi, W. Benstaali, B. Bouhafs, A. Abbad and A. Zitouni, *Effect of Coulomb interactions and Hartree-Fock exchange on structural, elastic, optoelectronic and magnetic properties of Co_2MnSi Heusler: A comparative study*, J. Magnetism and Magnetic Materials, 419, 74 (2016); https://doi.org/10.1016/j.jmmm.2016.06.012.
[34] S. Sharma, A. S. Verma and V. K. Jindal, *Ab initio studies of structural, electronic, optical, elastic and thermal properties of silver gallium dichalcogenides ($AgGaX_2$: X=S, Se, Te)*, Materials Research Bulletin, 53, 218 (2014); https://doi.org/10.1016/j.materresbull.2014.02.021.
[35] C. M. I. Okoye, *Theoretical study of the electronic structure, chemical bonding and optical properties of $KNbO_3$ in the paraelectric cubic phase*, J. Physics: Condensed Matter, 15, 5945 (2003); https://doi.org/10.1088/0953-8984/15/35/304.
[36] S. A. Korba, H. Meradji, S. Ghemid, B. Bouhafs, *First Principles calculations of structural, electronic and optical properties of $BaLiF_3$*, Compt. Mater. Science, 44, 1265 (2009); https://doi.org/10.1016/j.commatsci.2008.08.012.
[37] J. Sun, H. T. Wang, N. B. Ming, J. He and Y. Tian, *Optical properties of hetero diamond B_2CN using first-principles calculations*, Applied physics letters, 84, 4544 (2004); https://doi.org/10.1063/1.1758781.
[38] B. Mayer, H. Anton, E. Bott, M. Methfessel, J. Sticht, J. Harris, & P. C. Schmidt, *Ab-initio calculation of the elastic constants and thermal expansion coefficients of Laves phases*, Intermetallics, 11, 23 (2003); https://doi.org/10.1016/S0966-9795(02)00127-9.
[39] H. Fu, D. Li, F. Peng, T. Gao, & X. Cheng, *Ab initio calculations of elastic constants and thermodynamic properties of NiAl under high pressures*, Computational Materials Science, 44, 774 (2008); https://doi.org/10.1016/j.commatsci.2008.05.026.
[40] S. F. Pugh, *Relations between the elastic moduli and the plastic properties of polycrystalline pure metals*, The London, Edinburgh, and Dublin Philosophical Magazine and Journal of Science, 45, 823 (1954); https://doi.org/10.1080/14786440808520496.
[41] R. Hill, *The elastic behaviour of a crystalline aggregate*, Proceedings of the Physical Society Section A, 65, 349 (1952); https://doi.org/10.1088/0370-1298/65/5/307.
[42] M. S. Yaseen, G. Murtaza, & R. M. A. Khalil, *Ab-initio study of Li based chalcopyrite compounds $LiGaX_2$ (X= S, Se, Te) in tetragonal symmetry: A class of future materials for optoelectronic applications*, Current Applied Physics, 18, 1113 (2018); https://doi.org/10.1016/j.cap.2018.06.008.

Дж. Кумарі, Ч. Сінг[2], Б.Л. Чоудхарі[1], А.С. Верма[3,4]

Дослідження з перших принципів фізичних властивостей і стабільності напівпровідників халькопіриту на основі літію: надійність екологічних джерел енергії

[1]*Фізичний факультет, Банасталі Відьяпіт, Раджастхан, Індія*
[2]*Фізичний факультет, коледж Агри, Агра, Індія,*
[3]*Відділ досліджень та інновацій, факультет прикладних наук та наук про життя, Університет Уттаранчал, Дехрадун, Уттаракханд, Індія*
[4]*Університетський центр досліджень і розвитку, факультет фізики, Університет Чандігарха, Мохалі, Пенджаб, Індія,*
ajay_phy@rediffmail.com

У роботі на основі досліджень з перших принципів виконано розрахунки фізичних властивостей, структурних, електронних, оптичних і механічних властивостей літій-галієвих халькопіритів $LiGaX_2$ (X= S, Se). Використано два обмінні кореляційні потенціали, один – метод плоских хвиль з повним розширеним потенціалом (FP-LAPW), другий – метод псевдопотенціалу. Параметри гратки, зазначені в роботі, коливаються від a = b = 5,28 Å до 5,82 Å і c = 10,11 Å до 11,25 Å. Встановлено, що ці матеріали мають пряму заборонену зону 4,41 еВ для $LiGaS_2$ і 2,90 еВ для $LiGaSe_2$. Показники заломлення n(ω) для цих сполук становлять 2,1 і 2,3 відповідно. Вивчення оптичних і пружних властивостей цих матеріалів гарантує, що вони демонструють анізотропну поведінку та пластичні властивості.

Ключові слова: халькопірити; електронні властивості; оптичні властивості; пружні властивості.